ACS APPLIED MATERIALS & INTERFACES

Letter

www.acsami.org

3D Micropatterned Surface Inspired by *Salvinia molesta* via Direct Laser Lithography

Omar Tricinci,*[,†] Tercio Terencio,[†,#] Barbara Mazzolai,[†] Nicola M. Pugno,[‡,§,∥] Francesco Greco,*[,†] and Virgilio Mattoli*[,†]

[†]Center for Micro-BioRobotics, Istituto Italiano di Tecnologia, Viale Rinaldo Piaggio 34, 56025 Pontedera, Italy

[‡]Laboratory of Bio-inspired & Graphene Nanomechanics, Department of Civil, Environmental and Mechanical Engineering, University of Trento, via Mesiano 77, 38123 Trento, Italy

[§]Center for Materials and Microsystems, Fondazione Bruno Kessler, via Sommarive 18, 38123 Povo, Italy

[∥]School of Engineering & Materials Science, Queen Mary University of London, Mile End Road, London E1 4NS, United Kingdom

[#]Department of Neuroscience and Brain Technologies, Istituto Italiano di Tecnologia, Via Morego 30, 16163 Genoa, Italy

Supporting Information

ABSTRACT: Biomimetic functional surfaces are attracting increasing attention for their relevant technological applications. Despite these efforts, inherent limitations of microfabrication techniques prevent the replication of complex hierarchical microstructures. Using a 3D laser lithography technique, we fabricated a 3D patterned surface bioinspired to *Salvinia molesta* leaves. The artificial hairs, with crownlike heads, were reproduced by scaling down (ca. 100 times smaller) the dimensions of natural features, so that microscale hairs with submicrometric resolution were attained. The micropatterned surface, in analogy with the natural model, shows interesting properties in terms of hydrophobicity and air retention when submerged by water, even if realized with a hydrophilic material. Furthermore, we successfully demonstrated the capability to promote localized condensation of water droplets from moisture in the atmosphere.

KEYWORDS: *biomimetics, 3D laser lithography, hydrophobic surface, air trapping, fog collecting*

Nature provides a wide range of surfaces with many useful functions and properties, in both the animal and plants worlds.[1−7] Biomimetic smart surfaces for several practical applications can be derived from the study of biological surfaces. Typical examples of fascinating surface properties from the plants world are self-cleaning and superhydrophobicity, the so-called Lotus effect.[8,9] The study of hydrophobic surfaces has attracted considerable interest in recent years,[10−16] along with several efforts to produce artificial biomimetic superhydrophobic surfaces.[17−21]

In the present work, we report about a new type of artificial surface, three-dimensionally patterned at the micro- and nanoscale, and having a morphology inspired by the structure of the *Salvinia molesta* leaf. This plant is a floating fern, which possesses the remarkable property of long-term air retention on the surface of the leaves, when submerged in water, because of the peculiar microstructure and the related high hydrophobicity. The leaves of this plant have been thoroughly investigated from a morphological and functional point of view.[22−28] The upper side of leaves is covered with hairs capped with a crownlike (or "eggbeater") structure (Figure 1a); each hair is composed by a stalk, up to 1.5 mm long, bearing on the tip four rounded filaments which are connected at the apex, thus forming a crownlike structure of about 500 μm in height (Figure 1b). The overall multicellular hair structure, except for the apex, is covered with wax crystals with low surface energy and high roughness at the micronanoscale which provide high hydrophobicity. The apex is instead composed by a small group of dead cells, rather smooth and hydrophilic, which ensures an anchoring point for water droplets. Thanks to this complex morphology, the plant is able to retain an air layer when submerged in water, ensuring transpiration and insulation, which permits its survival during flooding. In more detail, according to more recent studies in the field, the long-term stability of the air film is given by the following five surface characteristics: hydrophobicity; presence of microscale or millimeter scale hairs; presence of additional fine structures (e.g., ridge, hairs or waxes); micro- and nanocavities; elasticity of the structures.[2,15]

Anyhow, among other properties, the hydrophobicity is the starting necessary condition to have the air trapping effect. The most notable aspect of hydrophobicity is that it does not merely depend upon chemical interaction between the solid surface and the liquid phase, but mostly on the superficial texture which provides a functional roughness at the micro- and nanoscale.[15,22] Moreover, there are experimental evidence that

Received: August 19, 2015
Accepted: November 11, 2015
Published: November 11, 2015

DOI: 10.1021/acsami.5b07722
ACS Appl. Mater. Interfaces 2015, 7, 25560−25567

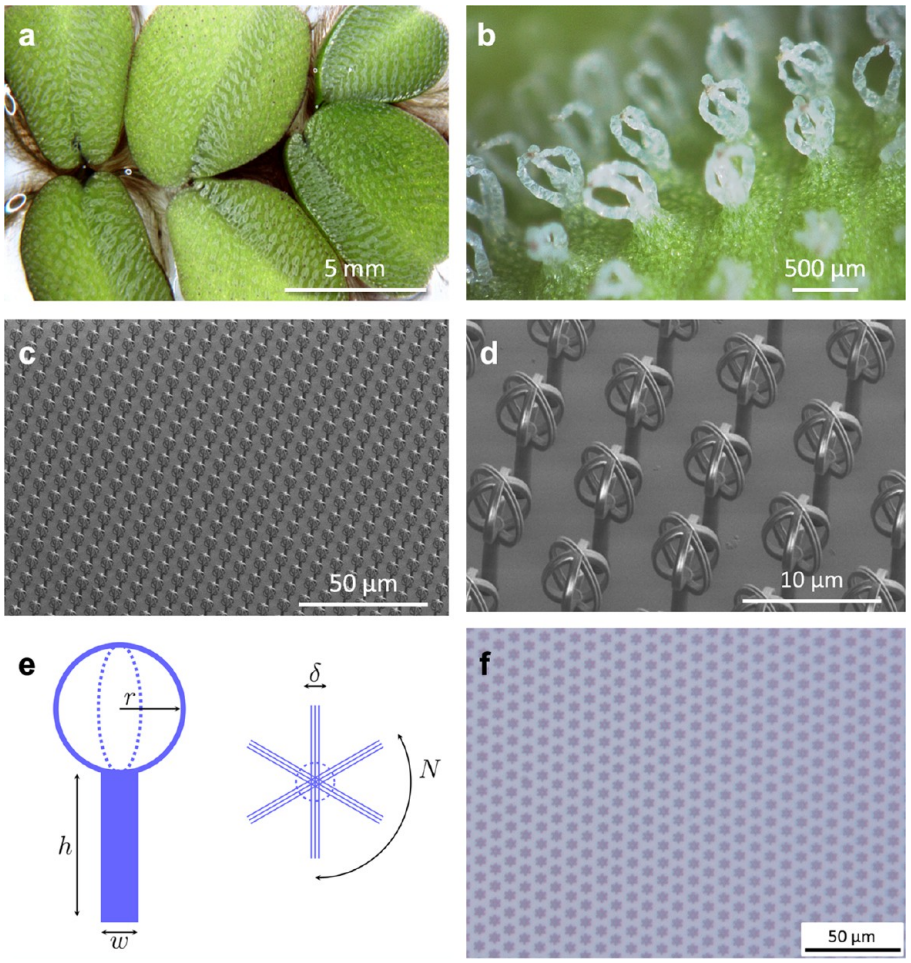

Figure 1. (a) Upper surface of *Salvinia molesta* leaf covered with hydrophobic hairs. (b) Detail of *Salvinia molesta* crownlike hairs. (c) Artificial crownlike hairs made in IP-DiLL photoresist on glass by means of 3D direct laser lithography. (d) Detail of artificial crownlike hairs on glass. (e) Scheme of artificial microhairs design with geometrical parameters (h and w are height and diameter of the stalk, whereas N and δ are the number of the filaments of the head and their thickness respectively). (f) Hexagonal arrangement of the array of artificial microhairs.

even a hydrophilic material (with high free surface energy) can macroscopically behave as hydrophobic if its surface has proper micro-nanostructured features.[29]

In this work, we focus on this aspect: starting from a hydrophilic material (a cross-linked epoxy-based photoresist), we propose a salvinia-inspired surface composed by micro-fabricated artificial hairs combined with a proper arrangement in arrays, able to show highly hydrophobic behavior. We investigated in particular how the morphology can affect the functional properties of the surface (hydrophobicity and air retention) as first step to develop surfaces with tailorable features. The implementation of such complex type of structured surfaces in artificial materials could be of great technological interest because it could allow the integration of different properties onto the same surface, just by tuning the arrangement and the morphology of the patterns.

To obtain artificial surfaces with interesting structure-related functions, we replicated the complex structure of *Salvinia molesta* hairs by downscaling it to the microscale. Such artificial surfaces were created by using 3D direct laser lithography. This technique, based on multiphoton absorption, allows to realize outstanding three-dimensional structures with features at the nanoscale, and it recently emerged as a powerful tool for fabricating 3D micropatterned surfaces for optics, photonics, as well as for bioinspired cell culture scaffolds.[30] Here we extended the range of applications of the technique to multifunctional plant-inspired surfaces, which are almost impossible to be replicated at such scale and with necessary resolution by other fabrication techniques.

Indeed, even if the replication of hydrophobic surfaces is quite common, the realization and the study of complex hierarchical three-dimensional structures have not been investigated yet, mainly due to serious limitations of available fabrication techniques. In this sense 3D laser lithography offers unique opportunity in the cross-disciplinary field of bioinspiration and biomimetics.

In the present work, artificial hairs were purposely designed about 100 times smaller than the natural ones (Figure 1c, d). The reason for downscaling the dimensions of the structures was related to the possibility to exploit the microscale physics to obtain behaviors not achievable at bigger scale. In particular, as demonstrated in the following, such small dimensions are required to obtain the targeted effect i.e. the obtainment of a surface with tunable hydrophobicity starting from a single hydrophilic material. Artificial hairs fabricated via direct laser lithography are composed by a cylindrical stalk and by a head mimicking the "eggbeater" structure of the *Salvinia molesta* leaves. The stalk of an artificial hair has a height of 7 μm and a diameter of 1.5 μm, whereas the head is obtained by intersecting three circumferences, rotated by 60° one from

DOI: 10.1021/acsami.5b07722
ACS Appl. Mater. Interfaces 2015, 7, 25560−25567

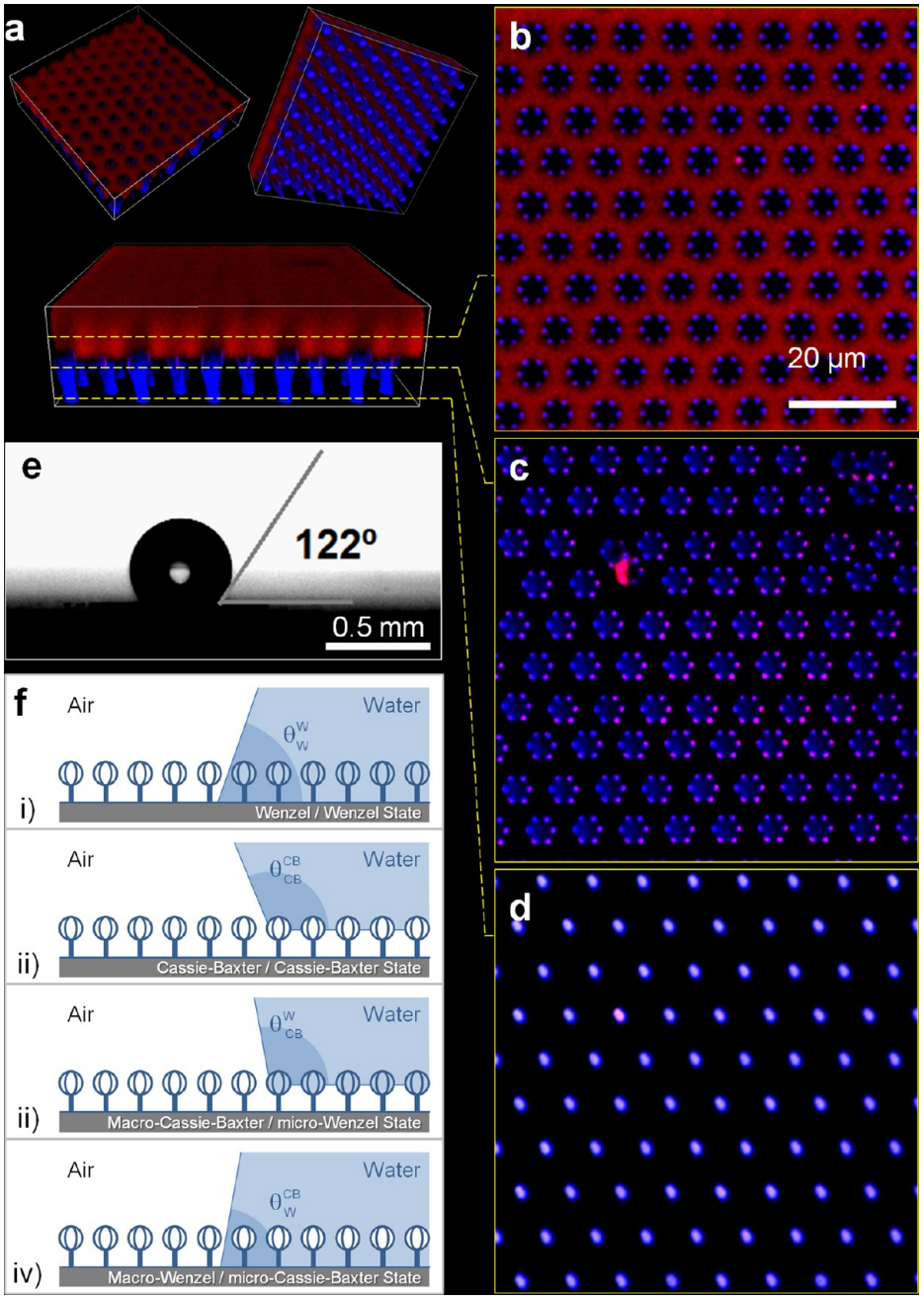

Figure 2. Salvinia-like micropatterned surface shows the capability of air trapping (water is colored in red, the structures in blue, air in black). (a) 3D reconstruction (from the images obtained with a confocal microscope) of a portion of the micropatterned surface showing the presence of air inside the crownlike hairs and between the stalks. Detail of a horizontal section of the micropatterned surface: (b) at the top level of the crownlike heads, (c) at the bottom level of the crownlike structure, and (d) at the level of the stalks. (e) Static contact angle test demonstrates the hydrophobicity of the artificial salvinia-like surface. (f) Schematic representation of the water-surface interface following (i) W-W, (ii) CB-CB, (iii) CB-W, and (iv) W-CB states, eqs 2−5).

the other, with a diameter of 6 μm and a thickness of 1 μm (Figure 1d, e). The arrays of artificial hairs, used in the tests, were arranged by following a 2D hexagonal lattice structure with a spacing of 9 μm between first-neighbor stalks and a minimum space between the head filaments of different hairs of about 3 μm (Figure 1f).

Thanks to the good mechanical properties of the cross-linked negative tone photoresist, the laser written structures were stable and the suspended crown-like head did not collapse even after submerging in water. Moreover, despite their tiny size and high aspect ratio, artificial hairs were well-anchored to the glass substrate, thanks to the optimization of the laser writing process.

To characterize the air trapping capability of salvinia-inspired surface, we implemented a dedicated experimental setup, based on the use of a confocal microscope (C2 Confocal Microscope System, Nikon), to detect the presence of water (suitably marked with the fluorescent probe TRITC) or air inside the crownlike heads and between the stalks (see also "Air trapping test" in the Supporting Information). It was possible to selectively detect and distinguish the artificial hair structure, the water and the air, which are respectively colored in blue, red

DOI: 10.1021/acsami.5b07722
ACS Appl. Mater. Interfaces 2015, 7, 25560−25567

and black in Figure 2. Indeed, the IP-DiLL photoresist itself is fluorescent if excited at 401 nm, whereas it is much less fluorescent at the excitation wavelength of TRITC (561 nm), where water marked with TRITC fluorescent probe is instead evidenced. In this way, it was possible to evaluate at microscopic level the interface between water, air, and the salvinia-inspired structures.

Notably, the artificial salvinia-like patterns demonstrated the capability to create an apparently stable air layer, trapped between the glass substrate and the hairs heads (see Figure 2a–d), thus partially reproducing the air trapping behavior of the natural counterpart. It is important to highlight that the design parameters of the hair head, in terms of its size, thickness, and number of circles that compose it, are a crucial aspect because they determine the number of solid–liquid and solid–air interfaces, thus conditioning the capacity of holding air under the hairs head. Indeed optimization of design went through several iterations, with different configurations tested before finding the suitable one (see the Supporting Information for some examples). Moreover, it should be noted that, even those designs that are not capable of air layer retention, stably trapped air inside the crown-like artificial structures, also at large crown diameters (see the Supporting Information). This fact could play an important role in terms of surface properties for tailoring specific functionalities.

Because the proposed artificial surface is able to trap air, the same should behave as a hydrophobic surface, even if the component materials (epoxy-based resist and glass) have high surface free energy and hydrophilic behavior on flat configuration. To verify this hypothesis, we evaluated the wettability of the surface, measuring the static water contact angle (CA) by means of an optical tensiometer (Attension Theta, Biolin Scientific). A larger patterned surface was specifically prepared to this purpose. Arrays were fabricated in the form of the square array with lateral size 900 μm (120 × 100 array). A droplet of deionized water with a diameter of about 500 μm was placed on top of a square array of hairs (Figure 2e). The surface proved to be highly hydrophobic (while not yet superhydrophobic), since the static contact angle was 122° ± 1°. This is a remarkable result because the static contact angle of a droplet of water on a flat surface made with the same material, IP-DiLL photoresist, was measured to be around 53° ± 1° with a contact angle hysteresis (CAH) of about 40° (in the range 65–25°, evaluated by drop evaporation method).[31]

From a theoretical point of view the contact angle (θ) of a liquid (water in our case) on a flat surface is related to the surface free energy of the solid composing that surface (γ_S), the liquid surface tension (γ_L) and the solid–water interfacial energy (γ_{SL}), by the well-known Young equation[32]

$$\gamma_W \cos(\theta) = \gamma_S - \gamma_{SL} \tag{1}$$

If the surface presents some degrees of roughness the previous equation is not valid any longer and the apparent (macroscopic) contact angle ($\theta^W{}_W$) can be expressed as a function of θ by the Wenzel equation[32]

$$\cos(\theta^W{}_W) = R\cos(\theta) \tag{2}$$

where the roughness parameter R is given by the ratio between the real surface area and the projected area. Wenzel model predicts that hydrophobicity always increases with roughness if the pristine material is hydrophobic; on the other hand, hydrophilicity increases with roughness if the material is hydrophilic. This is true only if all of the liquid phase is in direct contact with the surface (see Figure 2f.i) (solid–liquid interface only). When air is somehow trapped between the solid and the liquid, the Wenzel model is not valid any longer, and a more accurate description of the phenomenon is given by the Cassie–Baxter equation[10] that considers both solid–liquid and liquid–air interface fractions of the overall interface (see Figure 2f.ii). In this case, the apparent contact angle ($\theta^{CB}{}_{CB}$) is given by

$$\cos(\theta^{CB}{}_{CB}) = F_{SL}\cos(\theta) - F_{LA} \tag{3}$$

where F_{SL} and F_{LA} represent, respectively, the fraction of solid–liquid interface and liquid–air interface. In presence of a solid rough surface eq 3 must be modified according to eq 2, namely

$$\cos(\theta^{W}{}_{CB}) = RF_{SL}\cos(\theta) - F_{LA} \tag{4}$$

Thus, this equation also applies to hierarchical or rough microstructured surfaces (see Figure 2f.iii), and well-describes even the superhydrophobic behavior ($\theta^W{}_{CB} > 150°$)[23] of such type of surfaces. Noteworthy, the eq 4 predicts a mixed state (lower/macro-Cassie–Baxter and upper/micro-Wenzel) (see Figure 2f.iii) and it is for our specific geometry valid substituting R with R^m, F_{SL} with $F_{SL\ M}$ and F_{LA} with $F_{LA\ M}$, where "m" stands for "micro" and "M" for "macro" (in the previous equations, only global quantities play a role). Interestingly eq 4 predicts a hydrophobic behavior of the structured surface ($\theta^W{}_{CB} > 90°$) even if $\theta < 90°$ (i.e., pristine hydrophilic material), if the following condition is satisfied[10]

$$F_{LA} \geq R\cos(\theta)/[1 + R\cos(\theta)]$$

Analogously, in case of eq 3 the same behavior is obtained when

$$F_{LA} \geq \cos(\theta)/[1 + \cos(\theta)]$$

Thus, eq 2 corresponds to a fully Wenzel state (W-W), eq 3 to a fully Cassie–Baxter state (CB-CB), and eq 4 to the mixed state macro-Cassie–Baxter and micro-Wenzel (CB-W), whereas the remaining state macro-Wenzel and micro-Cassie–Baxter (W-CB) would be described by[33,34] (see Figure 2f.iv)

$$\cos(\theta^{CB}{}_{W}) = (R_M - 1 + F_{WM})\cos(\theta) + (1 - F_{WM})(F_{SL}{}^m\cos(\theta) - F_{LA}{}^m) \tag{5}$$

where again "m" stands for "micro" and "M" for "macro" and being $F_{W\ M}$ (macro-Wenzel interface fraction) geometrically equivalent to $(1 - F_{SL\ M})$.

By applying the previous equations to our specific experimentally observed case of the CB-CB state, we found a $\theta^{CB}{}_{CB}$ in the range 120°–133° (depending on how interface surfaces are calculated, see the Supporting Information for calculation details), which is in good agreement with the measured contact angle of 122° (see Figure 2e), thus further confirming the presence of a CB-CB regime when our surface is in contact with water. Anyhow it is important to underline that Cassie–Baxter equation alone does not tell us anything about the stability of the wetting state, that of course depends on the sample geometry, chemical and thermodynamic properties of the surface, as well as on environmental conditions (i.e., hydrostatic and hydrodynamic pressure).[12,25,30,35] Considering our artificial salvinia-inspired structures (composed by a hydrophilic material), from a purely thermodynamic point of

DOI: 10.1021/acsami.5b07722
ACS Appl. Mater. Interfaces 2015, 7, 25560–25567

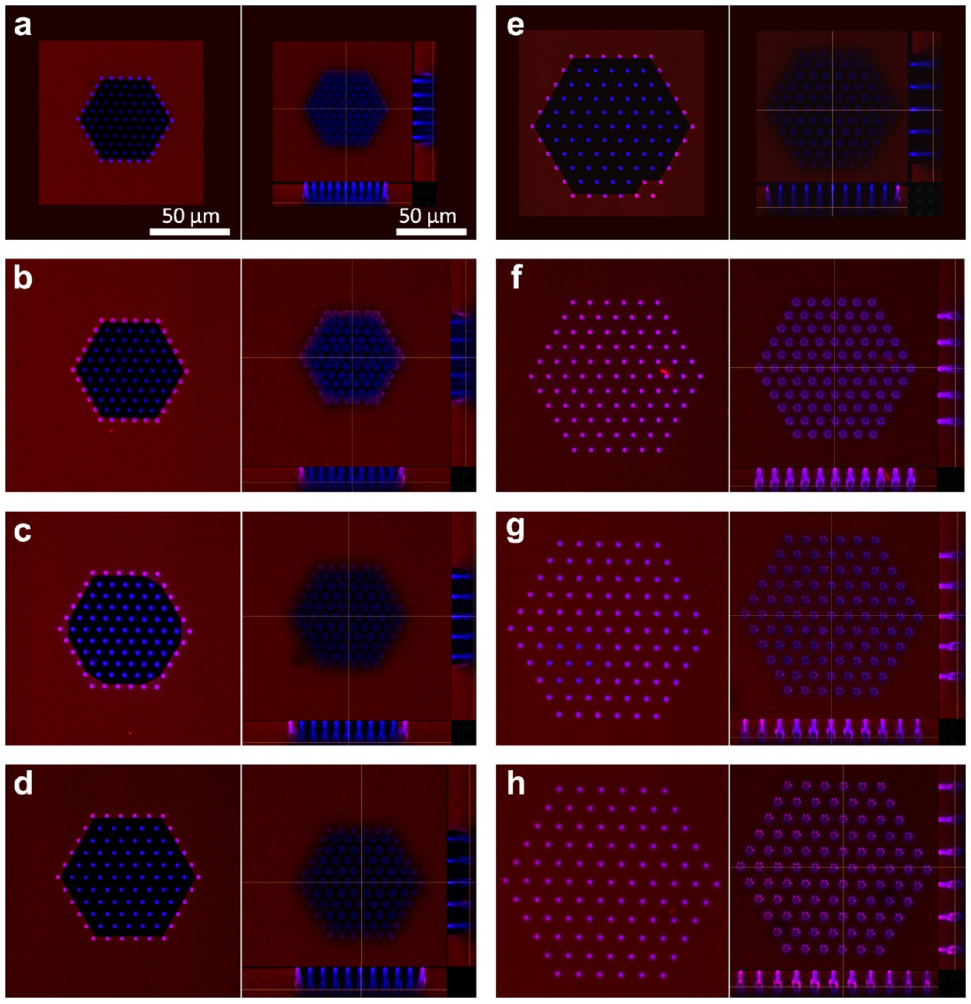

Figure 3. Air trapping test performed on a series of hexagonal samples with hexagonal arrangement of the stalks. The head-to-head distance varied from 0 to 7 μm (from a to h, with 1 μm increment per step). For each sample, different confocal microscope images are reported (water is colored in red, the structures in blue, air in black): the section at the level of the stalks, close to the glass substrate (on the left), the section at the level of the crown-like heads and the profile of the hairs (on the right). For a head-to-head distance between 4 and 5 μm (images in d, e), the switching between CB-CB and W-CB wetting regime occurs, whereas the air is always trapped inside the heads.

view the CB-CB state is always the higher energy state compared with W-W state, thus in principle disadvantaged. Nevertheless, the experimental evidence collected so far make us conclude that, despite the CB state would be disadvantageous, it happens that artificial structures behave like this. The persistence and thus the meta-stability of the CB-CB state has been verified to be at least in the order of hours in static conditions.

To further investigate this aspect we repeated air trapping tests on a series of samples with the same hair geometry (N = 3; r = 3 μm; δ = 1 μm; h = 7 μm; w = 1.5 μm), with a hexagonal array in hexagonal arrangement (6 hairs per side), by varying the head-to-head distance, from 0 to 7 μm (with steps of 1 μm). Results are reported in Figure 3. Interestingly, it appears that there is a threshold distance, in between 4 and 5 μm, at which the surface wetting regime switches between CB-CB to W-CB. This result indicates that the structure admits in certain conditions a metastable CB state. This behavior can be also motivated by the presence of a local minimum of the total interface energy when the air layer is formed, due to the particular geometry of the structure and in particular to the effect of re-entrant corners. In this condition, when the air layer is formed a certain amount of extra energy is required to overcome the energy barrier and further collapse in W-CB state (thermodynamically stable). This energy barrier must be proportional to the number of structures for unity of area. Increasing the interstalk distance this energy barrier decreases (while decreasing the density of stalks per unit of area), and the effect of gravity and pressure fluctuations could be sufficient for collapsing in W-CB state, as we experimentally observed. This suggests the robustness of the micro CB state always observed in our experiments even under W macroscopic condition, thus suggesting also that the scaling down of a *Salvinia* leaf may result in a similar robust functionality even using a hydrophilic material.

The provided interpretation is also in good agreement with the behavior of the proposed surface as related to vapor condensation. The condensation of liquid water from vapor on rough, microstructured, or superhydrophobic substrates is an interesting phenomenon since it induces a wetting behavior that is different from that of deposited water drops.[36] In particular, the growth dynamics of water droplets from vapor has been widely investigated in order to find a general model for this particular geometry-dependent property on different

DOI: 10.1021/acsami.5b07722
ACS Appl. Mater. Interfaces 2015, 7, 25560−25567

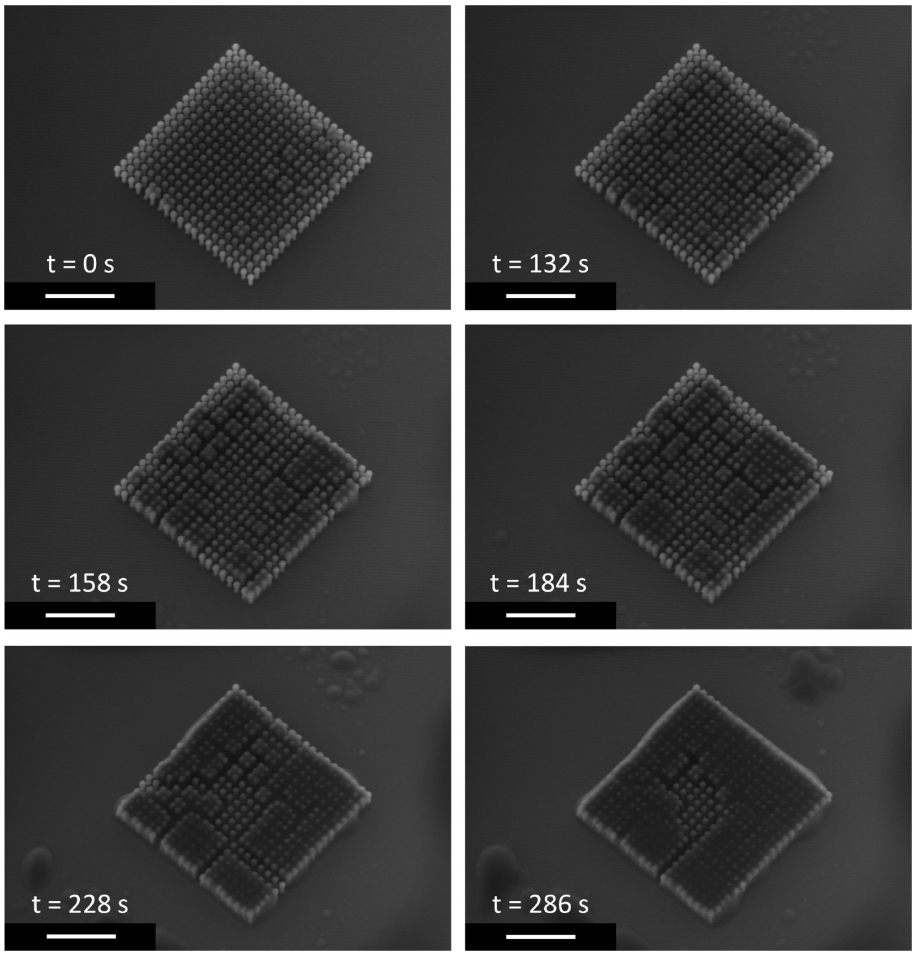

Figure 4. Environmental SEM images showing the temporal sequence of the water vapor condensation dynamics on the salvinia-like patterned surface (vapor pressure of 640 Pa, cooling stage temperature of 1.0 °C). The scale bar is 30 μm. The liquid water microdroplets nucleate around the crown-like heads and increase their size around the stalks, until they fill the entire space between the pillars and reach the substrate, according to the macro Wenzel regime. Finally, the water covers most of the salvinia-like array, forming a flat droplet.

substrates.[37−40] To assess the capability of our salvinia-inspired pattern in promoting the condensation of the water in the atmosphere, we carried out tests in an environmental scanning electron microscope (eSEM). To this purpose, salvinia-like hairs patterns were reproduced on a piece of silicon wafer. Silicon has been chosen because it provides a lower thermal resistance compared to the glass (see also "Water condensation test" in the Supporting Information). Even if the artificial hairs used in the previous tests showed the capability to support the nucleation of water droplets from the atmosphere (Figure S9 in the Supporting Information), the best results have been obtained by changing the design of the hairs. Such optimized structures shared the same salvinia-like general design, but had smaller features of the crown-like heads (N = 4 r = 2 μm; δ = 650 nm; h = 7 μm; square array 20 × 20 elements; stalk-to-stalk interdistance 5 μm) (Figure S8). The hairs were able to promote water condensation from environmental moisture. SEM micrographs acquired at different times permitted to appreciate the evolution of such condensation process. The liquid water microdroplets nucleated on the crown-like heads, characterized by a large number of solid−air interfaces, then droplets started growing (Figure 4). Indeed, the salvinia-like structure can be considered as a region where the roughness is much higher than that of the surrounding smooth silicon substrate and for this reason it represents a region of nucleation of the water droplets. As a result, a water layer is formed in macro W regime. This result, apparently in contrast with what discussed above, can be rationalized by considering that Wenzel regime is thermodynamically advantaged, and that the nucleation condensation process does not pass through the CB-CB metastable configuration.

Even if the proposed surface cannot be considered a "fog collector", because this type of behavior is typical of surfaces which are able also to promote the roll-off of collected water[41] (not verified in our case), the water condensation properties can be anyhow considered as an interesting starting point for further investigation. In particular, we believe that localized surface functionalization and fine-tuning of the geometrical parameters could be a viable step to reach the target of fog collection, which is particularly interesting in view of real technological applications.

In this Letter, we extended the use of 3D laser lithography based on two-photon polymerization of a negative photoresist to the fabrication of biomimetic surfaces. We demonstrated the fabrication of complex three-dimensional patterns with micro- and nanoscale features, replicating the morphology of the leaves of an aquatic fern, the *Salvinia molesta*, while downscaling its dimensions. The structure, made with a hydrophilic material, shows remarkable functional properties, such as air trapping, hydrophobicity, and promotion of localized water condensation

DOI: 10.1021/acsami.5b07722
ACS Appl. Mater. Interfaces 2015, 7, 25560−25567

from environmental moisture. It is possible to assume that the realization of different patterns on the same surface, in terms of geometry, dimension and spatial organization, can lead to a new type of functional structured surfaces, simply by modulating the entity of the three properties. Moreover, even if the microstructures presented in this work were fabricated on glass and silicon, there is no practical limitation in following the same procedure on a different substrate. Lastly, in addition to the technological applications of patterned surfaces with submicrometric resolution, the present work demonstrates for the first time the use of 3D laser lithography as a powerful tool for the investigation of wettability, air retention, and condensation phenomena, thus opening the way to more complex studies on how microscale morphology can affect macroscopic surface properties.

■ ASSOCIATED CONTENT

Supporting Information

The Supporting Information is available free of charge on the ACS Publications website at DOI: 10.1021/acsami.5b07722.

Some more details about surface fabrication, experimental procedures for air trapping and water condensation tests, and related figures (PDF)

■ AUTHOR INFORMATION

Corresponding Authors

*E-mail: omar.tricinci@iit.it.
*E-mail: francesco.greco@iit.it.
*E-mail: virgilio.mattoli@iit.it.

Notes

The authors declare no competing financial interest.

■ ACKNOWLEDGMENTS

The authors thank Mr. Carlo Filippeschi (Center for Micro-BioRobotics @SSSA, Istituto Italiano di Tecnologia) for the technical support and Mr. Giampiero Pallocca (Assing S.p.A. (Zeiss)) and Mr. Francesco Tatti (FEI Company) for eSEM imaging. N.M.P. is supported by the European Research Council (ERC StG Ideas 2011 BIHSNAM n. 279985 on "Bio-Inspired hierarchical supernanomaterials", ERC PoC 2013-1 REPLICA2 n. 619448 on "Large-area replication of biological antiadhesive nanosurfaces", ERC PoC 2013-2 KNOTOUGH n. 632277 on Supertough knotted fibers), by the European Commission under the Graphene Flag-ship (WP10 "Nanocomposites," n. 604391), and by the Provincia Autonoma di Trento ("Graphene Nanocomposites," n. S116/2012-242637 and delib. reg. n. 2266).

■ REFERENCES

(1) Bhushan, B. Biomimetics: Lessons from Nature - an Overview. *Philos. Trans. R. Soc., A* **2009**, *367*, 1445−1486.
(2) Koch, K.; Bhushan, B.; Barthlott, W. Multifunctional Surface Structures of Plants: an Inspiration for Biomimetics. *Prog. Mater. Sci.* **2009**, *54*, 137−178.
(3) Autumn, K.; Liang, Y. A.; Hsieh, S. T.; Zesch, W.; Chan, W. P.; Kenny, T. W.; Fearing, R.; Full, R. J. Adhesive Force of a Single Gecko Foot-hair. *Nature* **2000**, *405*, 681−685.
(4) Autumn, K.; Sitti, M.; Liang, Y. A.; Peattie, A. M.; Hansen, W. R.; Sponberg, S.; Kenny, T. W.; Fearing, R.; Israelachvili, J. N.; Full, R. J. Evidence for Van der Waals Adhesion in Gecko Setae. *Proc. Natl. Acad. Sci. U. S. A.* **2002**, *99*, 12252−12256.
(5) Kinoshita, S.; Yoshioka, S.; Kawagoe, K. Mechanisms of Structural Colour in the Morpho Butterfly: Cooperation of Regularity and Irregularity in an Iridescent Scale. *Proc. R. Soc. London, Ser. B* **2002**, *269*, 1417−1421.
(6) Dean, B.; Bhushan, B. Shark-skin Surfaces for Fluid-drag Reduction in Turbulent Flow: a Review. *Philos. Trans. R. Soc., A* **2010**, *368*, 4775−4806.
(7) Stavenga, D. G.; Foletti, S.; Palasantzas, G.; Arikawa, K. Light on the Moth-eye Corneal Nipple Array of Butterflies. *Proc. R. Soc. London, Ser. B* **2006**, *273*, 661−667.
(8) Barthlott, W.; Neinhuis, C. Purity of the Sacred Lotus, or Escape from Contamination in Biological Surfaces. *Planta* **1997**, *202*, 1−8.
(9) Neinhuis, C.; Barthlott, W. Characterization and Distribution of Water-repellent, Self-cleaning Plant Surfaces. *Ann. Bot.* **1997**, *79*, 667−677.
(10) Bhushan, B.; Jung, Y. C.; Koch, K. Micro-, Nano- and Hierarchical Structures for Superhydrophobicity, Self-cleaning and Low Adhesion. *Philos. Trans. R. Soc., A* **2009**, *367*, 1631−1672.
(11) Blossey, R. Self-cleaning Surfaces - Virtual Realities. *Nat. Mater.* **2003**, *2*, 301−306.
(12) Lafuma, A.; Quéré, D. Superhydrophobic States. *Nat. Mater.* **2003**, *2*, 457−460.
(13) Bhushan, B.; Jung, Y. C. Wetting, Adhesion and Friction of Superhydrophobic and Hydrophilic Leaves and Fabricated Micro/Nanopatterned Surfaces. *J. Phys.: Condens. Matter* **2008**, *20*, 225010.
(14) Bico, J.; Marzolin, C.; Quéré, D. Pearl Drops. *EPL Europhys. Lett.* **1999**, *47*, 220−226.
(15) Solga, A.; Cerman, Z.; Striffler, B. F.; Spaeth, M.; Barthlott, W. The dream of staying clean: Lotus and biomimetic surfaces. *Bioinspiration Biomimetics* **2007**, *2*, 126−134.
(16) Yan, Y. Y.; Gao, N.; Barthlott, W. Mimicking natural superhydrophobic surfaces and grasping the wetting process: A review on recent progress in preparing superhydrophobic surfaces. *Adv. Colloid Interface Sci.* **2011**, *169*, 80−105.
(17) Marzolin, C.; Smith, S. P.; Prentiss, M.; Whitesides, G. M. Fabrication of Glass Microstructures by Micro-molding of Sol-gel Precursors. *Adv. Mater.* **1998**, *10*, 571−574.
(18) Nosonovsky, M.; Bhushan, B. Biomimetic Superhydrophobic Surfaces: Multiscale Approach. *Nano Lett.* **2007**, *7*, 2633−2637.
(19) Öner, D.; McCarthy, T. J. Ultrahydrophobic Surfaces. Effects of Topography Length Scales on Wettability. *Langmuir* **2000**, *16*, 7777−7782.
(20) Jung, Y. C.; Bhushan, B. Mechanically Durable Carbon Nanotube-composite Hierarchical Structures with Superhydrophobicity, Self-cleaning, and Low-drag. *ACS Nano* **2009**, *3*, 4155−4163.
(21) Ebert, D.; Bhushan, B. Durable Lotus-effect Surfaces with Hierarchical Structure Using Micro- and Nanosized Hydrophobic Silica Particles. *J. Colloid Interface Sci.* **2012**, *368*, 584−591.
(22) Barthlott, W.; Schimmel, T.; Wiersch, S.; Koch, K.; Brede, M.; Barczewski, M.; Walheim, S.; Weis, A.; Kaltenmaier, A.; Leder, A.; Bohn, H. F. The Salvinia Paradox: Superhydrophobic Surfaces with Hydrophilic Pins for Air Retention Under Water. *Adv. Mater.* **2010**, *22*, 2325−2328.
(23) Koch, K.; Bohn, H. F.; Barthlott, W. Hierarchical sculpturing of plant surfaces and superhydrophobicity. *Langmuir* **2009**, *25*, 14116−14120.
(24) Grewal, H. S.; Cho, I. J.; Yoon, E. S. The role of bio-inspired hierarchical structures in Wetting. *Bioinspir. Biomim.* **2015**, *10*, 026009.
(25) Amabili, M.; Giacomello, A.; Meloni, S.; Casciola, C. M. Unraveling the Salvinia Paradox. *Adv. Mater. Interfaces* **2015**, *2*, 1500248.
(26) Ditsche, P.; Gorb, E.; Mayser, M.; Gorb, S.; Schimmel, T.; Barthlott, W. Elasticity of the hair cover in air-retaining Salvinia surfaces. *Appl. Phys. A: Mater. Sci. Process.* **2015**, *121*, 505−511.
(27) Barthlott, W.; Wiersch, S.; Čolić, Z.; Koch, K. Classification of trichome types within species of the water fern Salvinia, and ontogeny of the egg-beater trichomes. *Botany* **2009**, *87*, 830−836.
(28) Mayser, M. J.; Bohn, H. F.; Reker, M.; Barthlott, W. Measuring air layer volumes retained by submerged floating-ferns Salvinia and biomimetic superhydrophobic surfaces. *Beilstein J. Nanotechnol.* **2014**, *5*, 812−821.

DOI: 10.1021/acsami.5b07722
ACS Appl. Mater. Interfaces 2015, 7, 25560−25567

(29) Quéré, D. Wetting and Roughness. *Annu. Rev. Mater. Res.* **2008**, *38*, 71−99.
(30) Marino, A.; Filippeschi, C.; Mattoli, V.; Mazzolai, B.; Ciofani, G. Biomimicry at the nanoscale: Current research and perspectives of two-photon polymerization. *Nanoscale* **2015**, *7*, 2841−2850.
(31) Eral, H. B.; 't Mannetje, D. J. C. M.; Oh, J. M. Contact angle hysteresis: a review of fundamentals and applications. *Colloid Polym. Sci.* **2013**, *291*, 247−260.
(32) Israelachvili, J. N. *Intermolecular and Surface Forces*, 3rd ed; Academic Press: Waltham, MA, 2011.
(33) Pugno, N. In *The Nanomechanics in Italy*; Pugno, N., Ed.; Research Signpost: Kerala, India, 2007; Chapter 1, pp 1−9.
(34) Pugno, N. Towards a Spiderman suit: large invisible cables and self-cleaning releasable super-adhesive materials. *J. Phys.: Condens. Matter* **2007**, *19*, 395001.
(35) Konrad, W.; Apeltauer, C.; Frauendiener, J.; Barthlott, W.; Roth-Nebelsick, A. Applying methods from differential geometry to devise stable and persistent air layers attached to objects immersed in water. *Journal of Bionic Engineering* **2009**, *6*, 350−356.
(36) Dorrer, C.; Rụhe, J. Condensation and Wetting Transitions on Microstructured Ultrahydrophobic Surfaces. *Langmuir* **2007**, *23*, 3820−3824.
(37) Narhe, R. D.; Beysens, D. A. Water Condensation on a Superhydrophobic Spike Surface. *Europhys. Lett.* **2006**, *75* (1), 98−104.
(38) Narhe, R. D.; Beysens, D. A. Growth Dynamics of Water Drops on a Square-pattern Rough Hydrophobic Surface. *Langmuir* **2007**, *23*, 6486−6489.
(39) Jung, Y. C.; Bhushan, B. Wetting Behaviour During Evaporation and Condensation of Water Microdroplets on Superhydrophobic Patterned Surfaces. *J. Microsc.* **2008**, *229*, 127−140.
(40) Narhe, R. D.; Beysens, D. A. Nucleation and Growth on a Superhydrophobic Grooved Surface. *Phys. Rev. Lett.* **2004**, *93* (7), 076103.
(41) Azad, M. A. K.; Ellerbrok, D.; Barthlott, W.; Koch, K. Fog collecting biomimetic surfaces: Influence of microstructure and wettability. *Bioinspir. Biomim.* **2015**, *10*, 016004.

NOTE ADDED AFTER ASAP PUBLICATION

This paper was published on the Web on November 16, 2015. Additional text corrections were implemented, and the corrected version was reposted on November 25, 2015.

DOI: 10.1021/acsami.5b07722
ACS Appl. Mater. Interfaces 2015, 7, 25560−25567

Supporting information

3D Micropatterned Surface Inspired by *Salvinia molesta* via Direct Laser Lithography.

Omar Tricinci[*,†], *Tercio Terencio*[†,#], *Barbara Mazzolai*[†], *Nicola M. Pugno*[‡,§,‖], *Francesco Greco*[*,†], *Virgilio Mattoli*[*,†]

[†] Center for Micro-BioRobotics, Istituto Italiano di Tecnologia, Viale Rinaldo Piaggio 34, 56025 Pontedera, Italy

[#] Department of Neuroscience and Brain Technologies, Istituto Italiano di Tecnologia, Via Morego 30, 16163 Genoa, Italy

[‡] Laboratory of Bio-inspired & Graphene Nanomechanics, Department of Civil, Environmental and Mechanical Engineering, University of Trento, via Mesiano 77, 38123 Trento, Italy

[§] Center for Materials and Microsystems, Fondazione Bruno Kessler, via Sommarive 18, 38123 Povo, Italy

[‖] School of Engineering & Materials Science, Queen Mary University of London, Mile End Road, London E1 4NS, UK

Fabrication of Salvinia-Inspired Structures. The design of the salvinia-like structures (Figure 1e) has been programmed with Matlab® (The Mathworks, Inc.). Arrays of regularly arranged artificial hairs were realized in negative tone IP-DiLL photoresist (Nanoscribe GmbH) on a glass substrate, using a direct laser lithography setup, Photonic Professional system (Nanoscribe GmbH). At first the glass substrate has been rinsed with acetone, Isopropyl alcohol (IPA) and deionized water. A thin layer of few nanometers of Indium tin oxide (ITO) has been deposited on the substrate with a DC Magnetron sputtering system, at a power of 80W for 3 min. The ITO layer makes possible the detection of the interface between the substrate and the photoresist. It also ensures a good adhesion of the structures on the glass surface. Finally a drop of IP-DiLL photoresist has been cast on the substrate. The structures were fabricated by exposing the photoresist to a laser beam with a center wavelength of 780 nm, using a writing speed of 100 $\mu m\ s^{-1}$ with a power of 4.6 mW (Calman laser source). The sample was then developed for 20 min in SU-8 Developer (MicroChem Corp) and rinsed with IPA and deionized water.

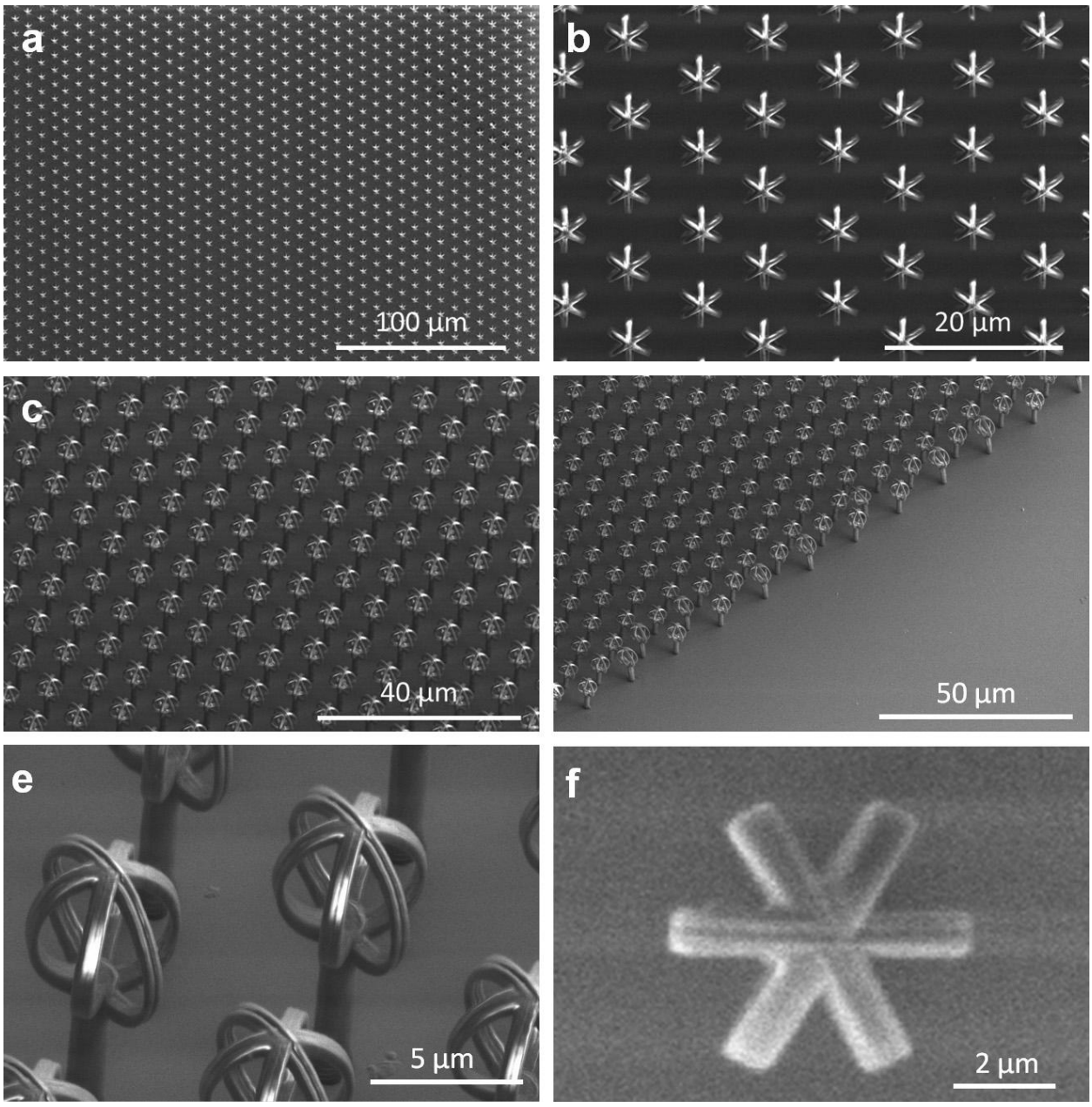

Figure S1. Additional SEM images of the sample presented in main text (square array of hairs with a head-to-head distance of 3 µm; hair parameter: N = 3; r = 3 µm; δ = 1 µm; h = 7 µm; *w* = 1.5 µm) at different magnifications and view angles.

Air trapping test details. In order to evaluate the air trapping capability and visualize the solid-liquid, solid-air and liquid-air interfaces, a confocal microscope (C2 Confocal Microscope System, Nikon) was used. The water used to submerge the sample was marked with a fluorescent probe, Tetramethylrhodamine-5-(and-6)-isothiocyanate (5(6)-TRITC) (Life Technologies), with a concentration of 0.01 mg mL^{-1} in water. The sample surface were observed at the confocal microscope by exciting at two different light wavelengths: 401 nm (excitation wavelength of IP-DiLL photoresist self-fluorescence) and 561 nm (excitation wavelength of TRITC).

All the analysis has been carried out by encapsulating the sample as in the following: a ring of silicone elastomer poly(dimethyl siloxane) (PDMS, Sylgard 184, Dow Corning Corp), with an internal diameter of 8 mm and a thickness of 200 μm, has been placed around the array of hairs on the glass, in order to confine the solution around the array and mainly to avoid optical aberrations due to the spherical shape of the droplet. The ring has been prepared by spin coating PDMS on a glass and then cutting it with a laser cutting system (Versalaser, Universal Laser Systems). After the deposition of the TRITC solution droplet with a volume of about 10 μL, a glass slide was put over the ring, sealing the sample.

Air trapping tests were carried out on different types of samples:

- Square arrays of about 180 μm per side (22x20 hairs) have been preliminary used to study the air trapping phenomenon, checking the presence of the air inside the crown-like heads and, in case, between stalks, by using different geometrical parameters. Only results on best samples (hair parameter: $N = 3$; $r = 3$ μm; $\delta = 1$ μm; $h = 7$ μm; $w = 1.5$ μm; head-to-head distance 3 μm), have been shown in the main text. Additional design and test results can be found in the following section.

- Hexagonal arrays with 6 hairs per side in hexagonal arrangement (hair parameter: $N = 3$; $r = 3$ μm; $\delta = 1$ μm; $h = 7$ μm; $w = 1.5$ μm) have been used for evaluating the capability of the arrangement of the structures in preventing the entrance of the water between the stalks, by modulating the head-to-head distance (varied from 0 to 7 μm, with steps of 1 μm).

Air trapping on different structures. Here we report additional pictures of air trapping tests on the main sample geometry (Figure S2 and S3) and on other samples with different geometrical parameters. (Figure S4-S6). Notably all the samples that are not able to keep an air layer, are anyhow capable of trapping air inside the crown-like structure.

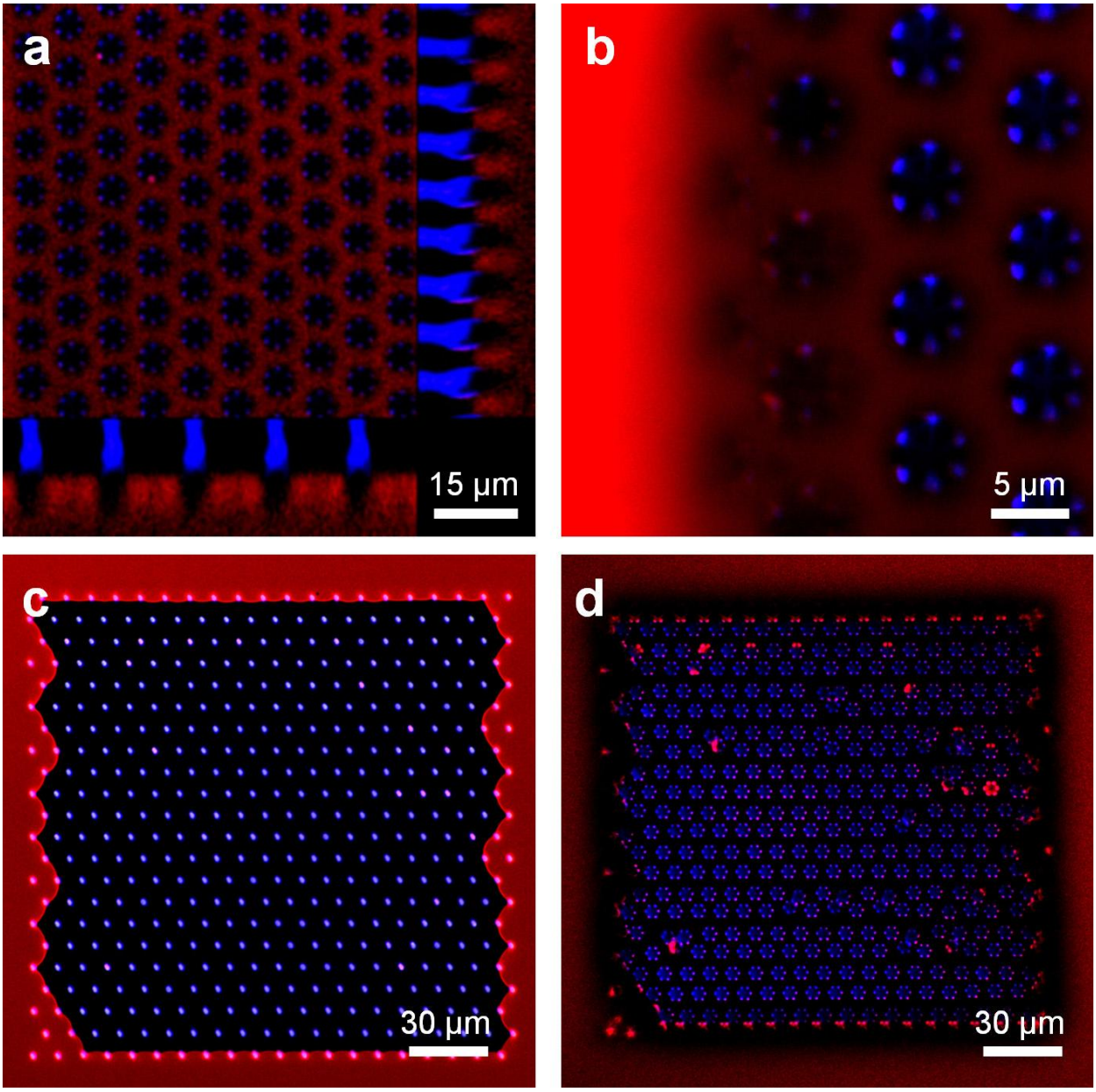

Figure S2. Additional confocal images of the sample presented in main text (square array of hairs with a head-to-head distance of 3 µm; hair parameter: $N = 3$; $r = 3$ µm; $\delta = 1$ µm; $h = 7$ µm; $w = 1.5$ µm). a) Section at the level of the crown-like heads and the profile of the hairs, showing the presence of air inside the heads. b) Detail of a section of the same micro-patterned surface close to the border of the array. Section of the whole micro-patterned surface at the level of the stalks (c) and at the level of the crown (d) showing the presence of trapped air.

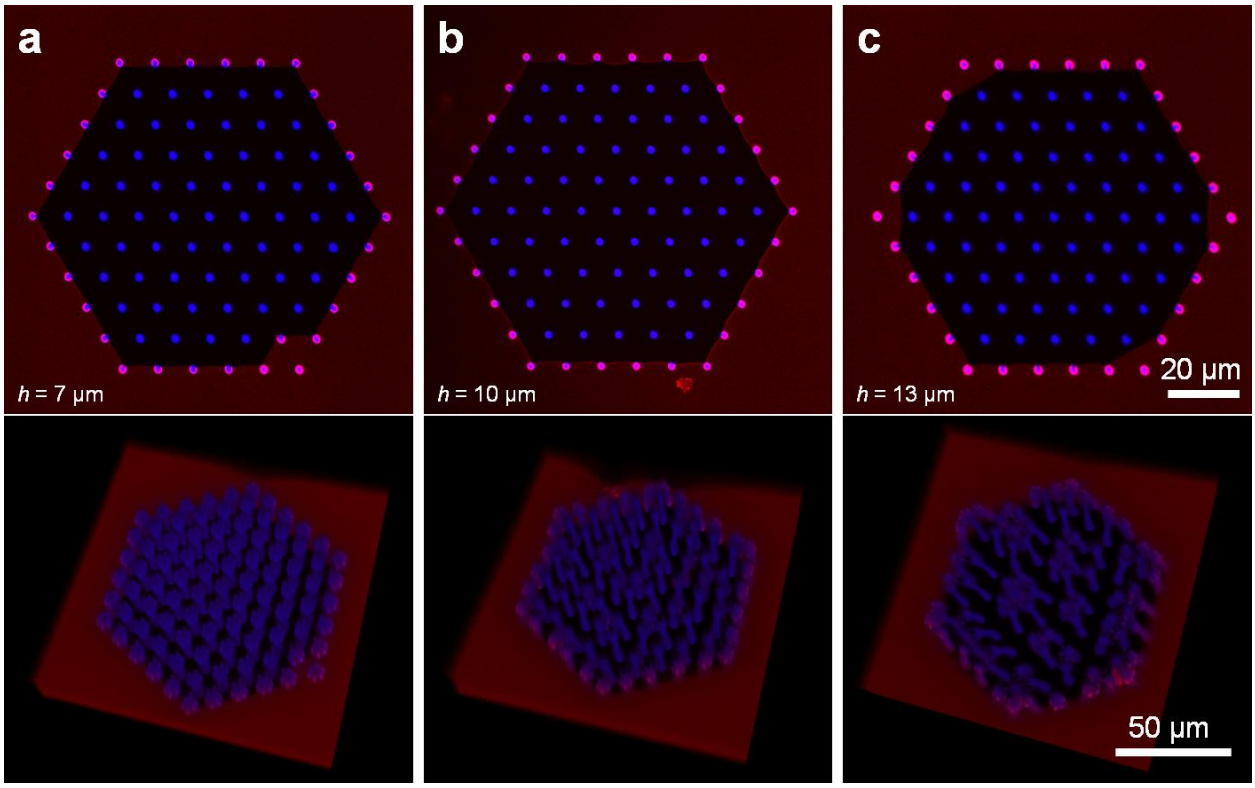

Figure S3. Trapping air test (sections and 3D reconstruction) performed on hexagonal arrays with variable stalk length: h = 7 µm (a), 10 µm (b), 13 µm (c). (Other hair parameters: N = 3; r = 3 µm; δ = 1 µm; *w* = 1.5 µm; head-to-head distance of 3 µm). Noticeably longer and bunched hairs are still able to trap the air inside the structure.

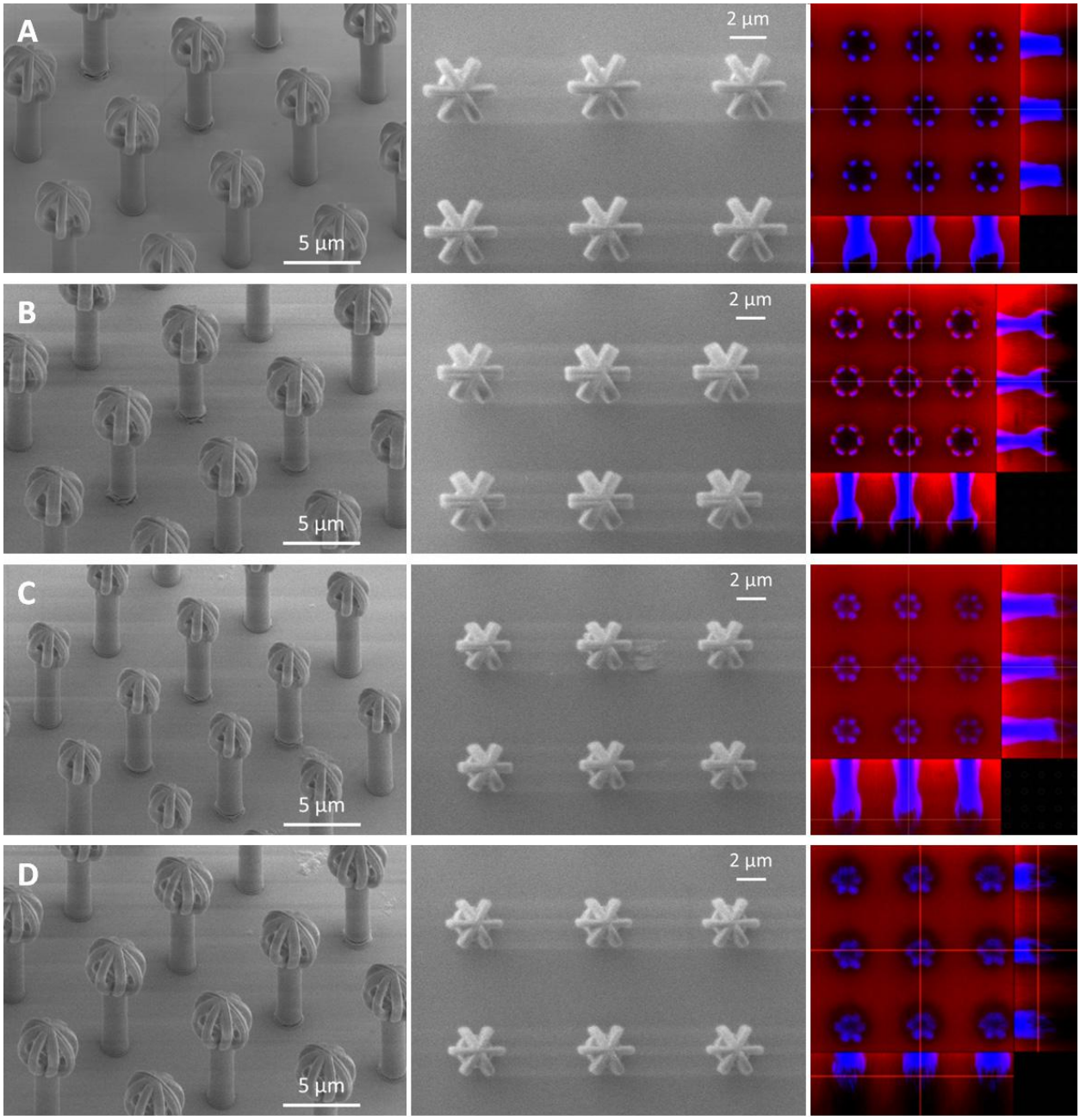

Figure S4. SEM images (left and center) and confocal images (right) of not-air trapping extra samples with following parameters:

Sample A - N = 3; r = 2 µm; δ = 0.65 µm; h = 7 µm; w = 1.5 µm stalk-to-stalk distance: 8 µm;

Sample B - N = 3; r = 2 µm; δ = 1 µm; h = 7 µm; w = 1.5 µm stalk-to-stalk distance: 8 µm;

Sample C - N = 3; r = 1.5 µm; δ = 0.63 µm; h = 7 µm; w = 1.5 µm stalk-to-stalk distance: 7 µm;

Sample D - N = 3; r = 1.5 µm; δ = 0.58 µm; h = 7 µm; w = 1.5 µm stalk-to-stalk distance: 7 µm.

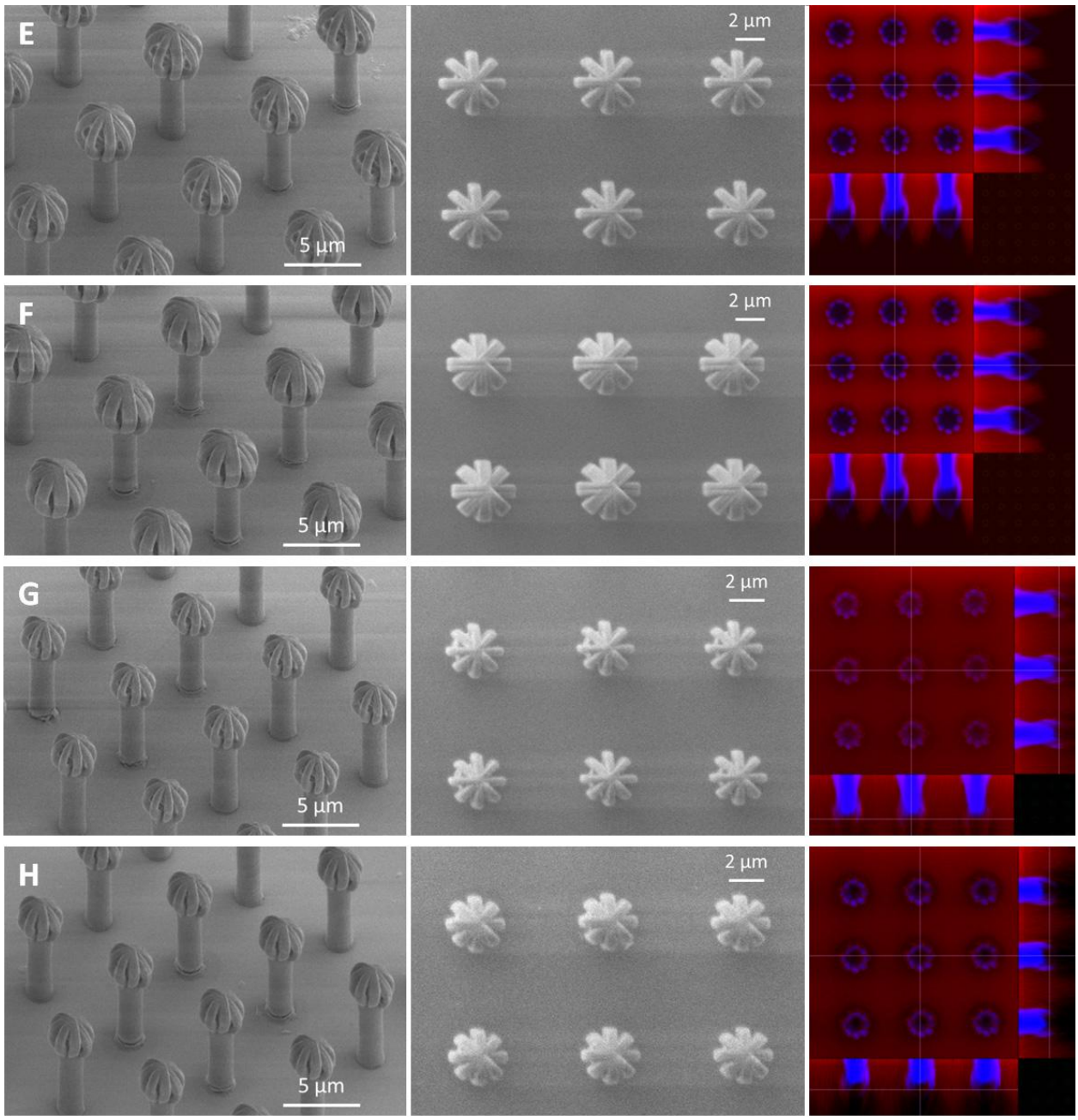

Figure S5. SEM images (left and center) and confocal images (right) of not-air trapping extra samples with following parameters:
Sample E - N = 4; r = 2 µm; δ = 0.66 µm; h = 7 µm; w = 1.5 µm stalk-to-stalk distance: 8 µm;
Sample F - N = 4; r = 2 µm; δ = 1 µm; h = 7 µm; w = 1.5 µm stalk-to-stalk distance: 8 µm;
Sample G - N = 4; r = 1.5 µm; δ = 0.49 µm; h = 7 µm; w = 1.5 µm stalk-to-stalk distance: 7 µm;
Sample H - N = 4; r = 1.5 µm; δ = 0.65 µm; h = 7 µm; w = 1.5 µm stalk-to-stalk distance: 7 µm.

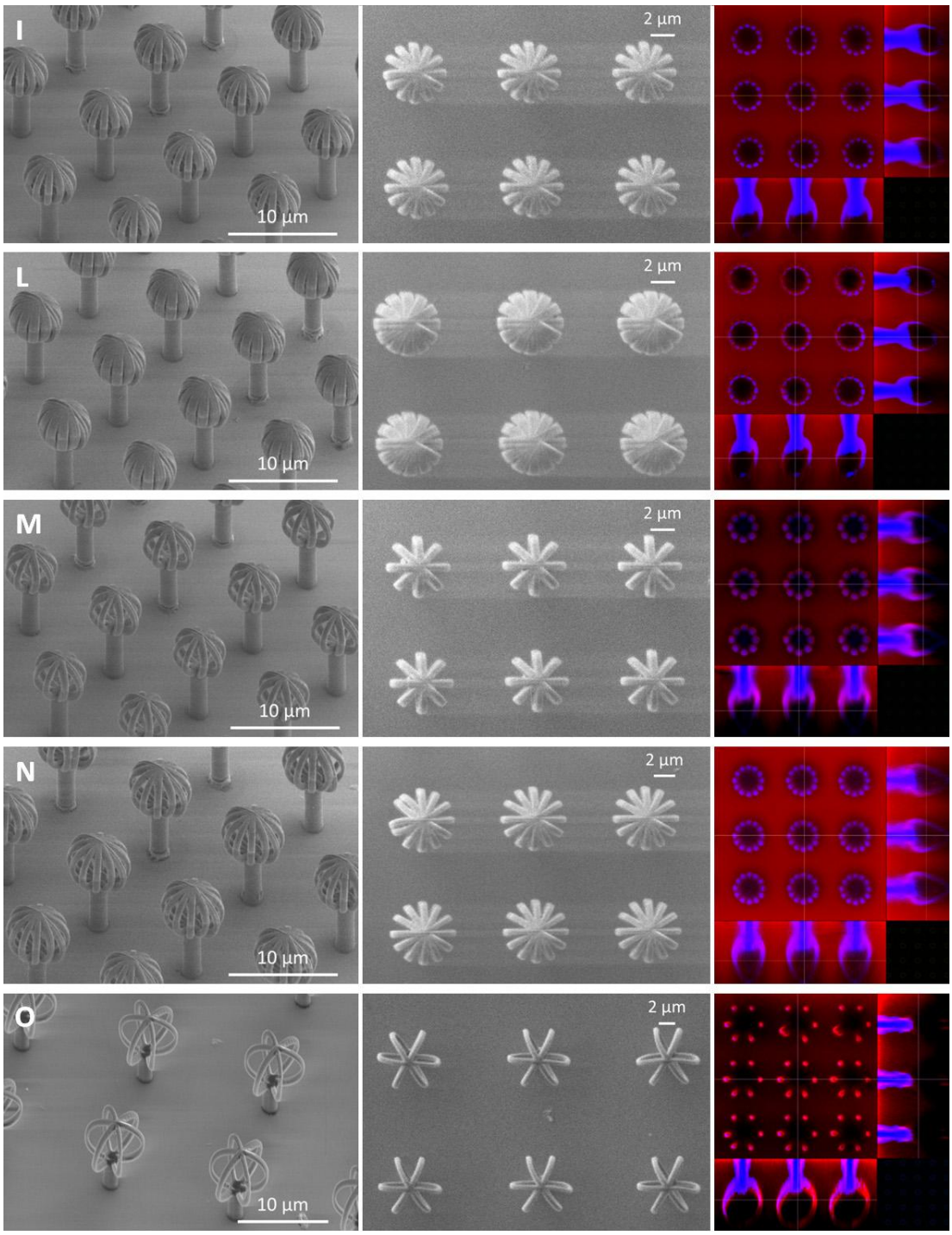

Figure S6. SEM images (left and center) and confocal images (right) of not-air trapping extra samples with following parameters:
Sample I - N = 6; r = 2.5 µm; δ = 0.7 µm; h = 7 µm; w = 1.5 µm stalk-to-stalk distance: 9 µm;
Sample L - N = 6; r = 2.5 µm; δ = 1 µm; h = 7 µm; w = 1.5 µm stalk-to-stalk distance: 9 µm;
Sample M - N = 4; r = 2.5 µm; δ = 0.68 µm; h = 7 µm; w = 1.5 µm stalk-to-stalk distance: 9 µm;
Sample N - N = 6; r = 3 µm; δ = 0.8 µm; h = 7 µm; w = 1.5 µm stalk-to-stalk distance: 10 µm;
Sample O - N = 3; r = 4 µm; δ = 0.75 µm; h = 7 µm; w = 1.5 µm stalk-to-stalk distance: 11 µm.

CB-CB CA calculation

CB-CB equation (2) estimates the macroscopic apparent contact angle (θ^{CB}_{CB}) of a liquid on a structured surface when air pockets are trapped in between liquid-solid interface. This is the experimentally observed state. Accordingly, predicted apparent contact angle (θ^{CB}_{CB}) is given by:

$$\theta^{CB}_{CB} = \arccos(F_{SL}\cos(\theta)–1 + F_{SL}) \quad (S1)$$

where F_{SL} represents the fraction of solid-liquid interface and $\theta = 53°$ is the contact angle of the pristine flat material composing the structured surface.

The interpretation of F_{SL} is not unique here due to the peculiar micro geometry of the crown-head. The simplest assumption is to calculate it as the projection of this structure on a horizontal plane divided by the area of the unitary hexagonal cell, basically assuming an equivalent cylindrical crown-head. This assumption would lead to $F_{SL} = 0.20$ and according to eq. S1 to $\theta^{CB}_{CB} = 133°$**.** On the other hand, considering the spherical geometry of the crown-head, F_{SL} could be estimated multiplying the previous estimation by the ratio of the real area of the crown-head in contact with water, nearly semispherical, and its projection; in this case we have $F_{SL} = 0.33$, leading to $\theta^{CB}_{CB} = 120°$**.** Note that the experimental observed CA is of 122° and is thus in between to these "limiting" predictions, but more close to the "semispherical" approximation that considers out-of-the-plane geometry.

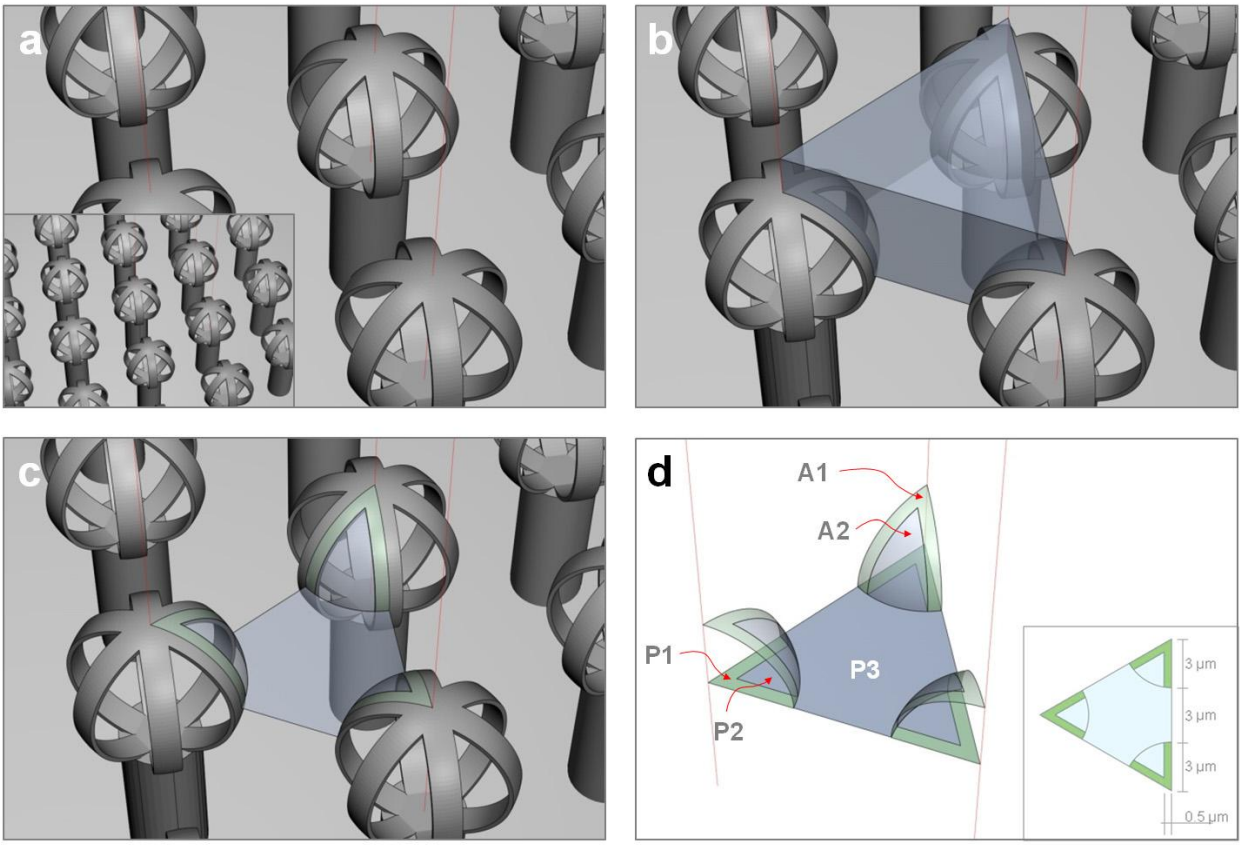

Figure S7. Schematic representation of the micro-structured surface (a) with highlighted the solid-liquid and liquid-air interfaces on a unitary cell (b-c); d) projection of the interfaces on the horizontal plane passing through the centers of crown structures. F_{SL} for equation (S1) is calculated in the first case (flat case) as F_{SL} = [3*P1/(3*P1+3*P2+P3)] = 0.20; in the second case F_{SL} = [3*A1/(3*P1+3*P2+P3)] = 0.33.

Water condensation test. For the final condensation analysis with the environmental scanning electron microscope, the sample (patterned following the previously described experimental procedure), was a square of silicon wafer with a side of 1 cm. It was put on a Peltier cell that provided cooling of sample at T = 1.0 °C and then placed in the eSEM chamber at a pressure of 640 Pa.

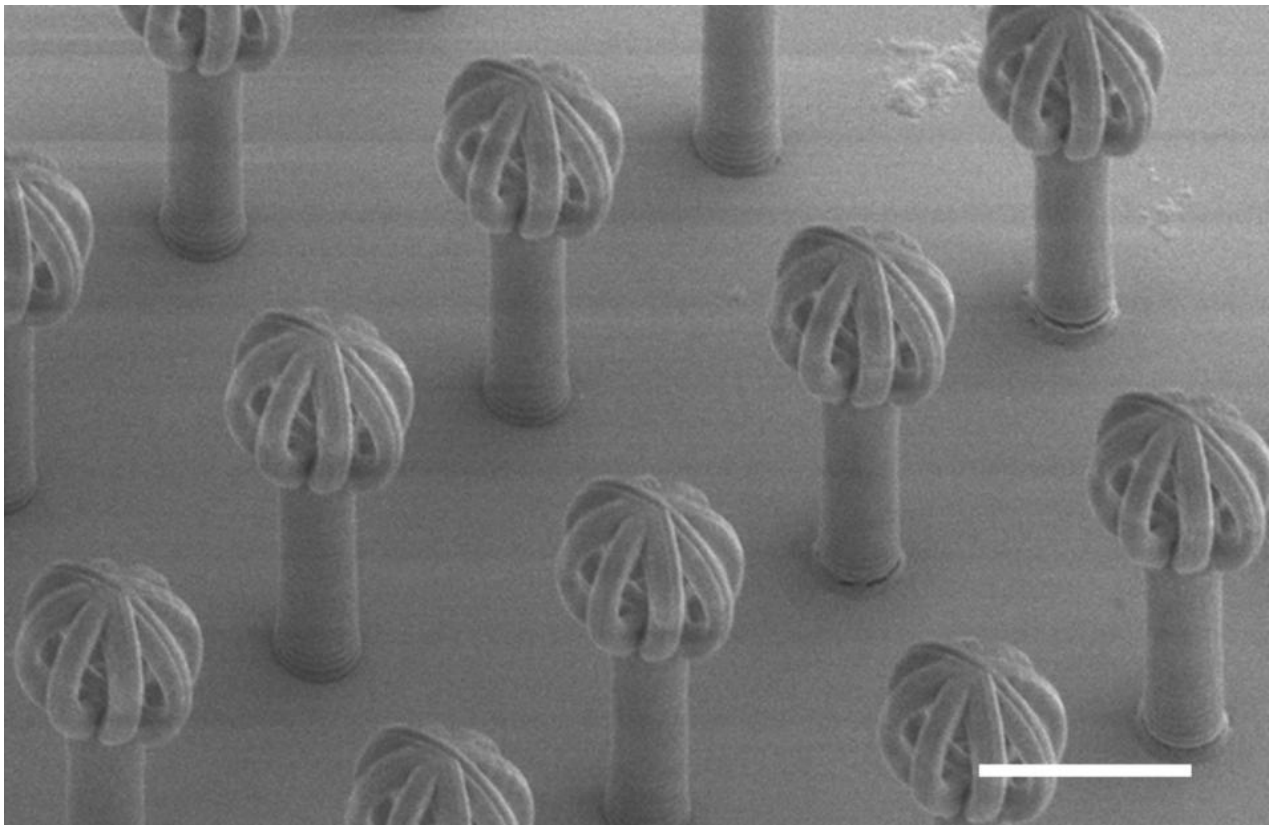

Figure S8. Artificial hairs used in the final condensation test. The diameter of the heads measures 4 μm while the thickness of its filaments is 650 nm. The full sample is composed by a square array of 20 x 20 elements: the distance between nearest neighbour elements (stalk to stalk) is 5 μm.

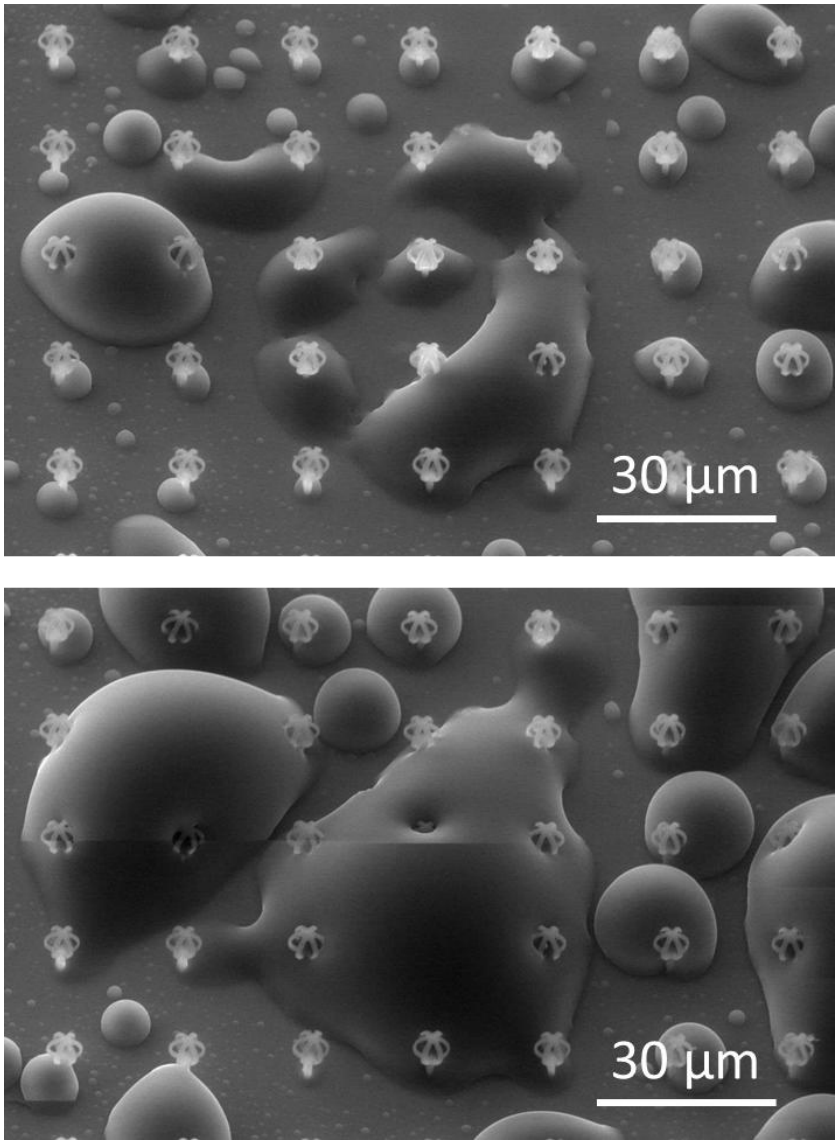

Figure S9. Extra condensation experiment on artificial hairs with head diameter of 6 µm and filaments thickness of 1 µm. The hairs are arranged in a square array with a distance of 20 µm between adjacent stalks. The vapor pressure in the chamber of the eSEM is 815 Pa and the cooling stage temperature is 3.0 °C.